3-29-2023

# Artificial neural network-based prediction assessment of wire electric discharge machining parameters for smart manufacturing

Itagi Vijayakumar Manoj

SannaYellappa Narendranath

Peter Madindwa Mashinini

Hargovind Soni

Shanay Rab

*See next page for additional authors*

## Authors

Itagi Vijayakumar Manoj, SannaYellappa Narendranath, Peter Madindwa Mashinini, Hargovind Soni, Shanay Rab, Shadab Ahmad, and Ahatsham Hayat

Research Article

Itagi Vijayakumar Manoj, SannaYellappa Narendranath, Peter Madindwa Mashinini, Hargovind Soni*, Shanay Rab, Shadab Ahmad, and Ahatsham Hayat*

# Artificial neural network-based prediction assessment of wire electric discharge machining parameters for smart manufacturing

https://doi.org/10.1515/pjbr-2022-0118
received December 13, 2022; accepted March 29, 2023

**Abstract:** Artificial intelligence (AI), robotics, cybersecurity, the Industrial Internet of Things, and blockchain are some of the technologies and solutions that are combined to produce "smart manufacturing," which is used to optimize manufacturing processes by creating and/or accepting data. In manufacturing, spark erosion technique such as wire electric discharge machining (WEDM) is a process that machines different hard-to-cut alloys. It is regarded as the solution for cutting intricate parts and materials that are resistant to conventional machining techniques or are required by design. In the present study, holes of different radii, *i.e.* 1, 3, and 5 mm, have been cut on Nickelvac-HX. Tapering in WEDM is a delicate process to avoid disadvantages such as wire break, wire bend, wire friction, guide wear, and insufficient flushing. Taper angles *viz.* 0°, 15°, and 30° were obtained from a unique fixture to get holes at different angles. The study also shows the influence of taper angles on the part geometry and area of the holes. Next, the artificial neural network (ANN) technique is implemented for the parametric result prediction. The findings were in good agreement with the experimental data, supporting the viability of the ANN approach for the evaluation of the manufacturing process. The findings in this research provide as a reference to the potential of AI-based assessment in smart manufacturing processes and as a design tool in many manufacturing-related fields.

**Keywords:** manufacturing, machining, EDM, cutting speed, dwell time, ANN

## 1 Introduction

Nickel alloys have good properties such as thermal stability, fatigue strength, corrosion resistance, and high-temperature strength. Industries such as aerospace, petrochemical, marine, food processing, and nuclear have demanded such nickel-based components. Conventional machining of nickel-based alloys leads to many defects in a tool such as flank wear, creator wear, edge chipping, and on machined surfaces such as grooves, surface cavities, crack, and microvoids [1]. As wire electric discharge machining (WEDM) removes the material by spark erosion technique, it is independent of the hardness of the material. Complex shapes of different materials such as nickel and cobalt superalloys, titanium-based alloys, ceramics, composites, nano-ceramics, and shape memory alloys can be machined using WEDM. The machining of nickel-based superalloys poses a major challenge for engineers due to their unique combination of properties, such as high toughness, heat resistance, hardness, strength-to-weight ratio, chemical reactivity with tool materials, low thermal conductivity, and limited creep resistance. Although these properties are crucial for the intended applications of these materials, the high temperatures and stresses that are generated during machining can lead to suboptimal machining performance and shorter tool life. As a result, unconventional

* **Corresponding author: Hargovind Soni,** Department of Mechanical Engineering, National Institute of Technology Delhi, Delhi, 110036, India, e-mail: hargovindsoni2002@gmail.com
* **Corresponding author: Ahatsham Hayat,** Department of Electrical and Computer Engineering, University of Nebraska-Lincoln, Lincoln, NE, USA, e-mail: aahatsham2@huskers.unl.edu

**Itagi Vijayakumar Manoj:** Department of Mechanical Engineering, Nitte Meenakshi Institute of Technology, Bengaluru 560064, Karnataka, 560064, India
**SannaYellappa Narendranath:** Department of Mechanical Engineering, National Institute of Technology Karnataka Surathkal, Surathkal, 575025, India
**Peter Madindwa Mashinini:** Department of Mechanical & Industrial Engineering Technology, University of Johannesburg, PO Box 524, Auckland Park, 2006, South Africa
**Shanay Rab:** School of Architecture, Technology, and Engineering, University of Brighton, Brighton BN2 4GJ, UK
**Shadab Ahmad:** School of Mechanical Engineering, Shandong University of Technology, Zibo 255000, China

machining methods, such as WEDM, may be required to meet the growing demands of the industry. The WEDM offers exceptional precision and accuracy [2–4]. Mouralova *et al.* [5] experimentally established that there was an optimum cutting speed from which a good surface quality component was obtained by machining in WEDM. Ming *et al.* [6] proposed a fusion thermo-physical model based on the finite element method to predict the machining performances of BN-AlN-$TiB_2$ with different weight proportions and to find the optimal process parameters. The novel model's accuracy was verified by comparing with experimental results, showing relative errors of 24.56, 16.16, and 1.87% in material removal rate, surface roughness, and kerf width, respectively. Additionally, a series of experiments were conducted to investigate the effects of process parameters on machining performances for WEDM of different BN-AlN-$TiB_2$ composite ceramics with 6, 8, and 10 wt% TiB2. He *et al.* [7] machined 2D C/SiC composite using WEDM, where the importance of surface roughness and machining speed was highlighted. Wang *et al.* [8] proposed a system capable of predicting corner errors and suggesting optimal machining parameters that can result in smaller corner errors and faster machining speeds compared to the original parameters. To validate the effectiveness of the proposed system, cutting experiments were conducted, and the results indicated a 20–39% improvement in corner accuracy. Tapering in WEDM is one of the important operations that help to meet the demand for complex manufacturing components. Kinoshita *et al.*, Martowibowo and Wahyudi, Yan *et al.*, Sanchez *et al.*, and Joy *et al.* [9–13] have adopted many taper techniques for avoiding the disadvantages of wire break, wire bend, insufficient flushing, guide wear, wire friction, *etc*. Manoj and Narendranath and Manoj *et al.* [14,15] examined the variation of profiling speed, surface roughness, micro-hardness, and recast layer for circular profile components at different taper angles. The authors have also investigated the effects of servo voltage, pulse on time, cutting speed override (CO), and pulse off time for the same material. Abyar *et al.* [16] claimed that 57% of the error was contributed by wire deflection in WEDM during machining. Bisaria and Shandilya [17] have utilized pulse modification techniques to improve the accuracy of corners at a right angle (90°), obtuse angle (120°), and acute angle (60°). Werner [18] experimentally determined optimal machining parameters and tool travel for machining curvilinear profiles by modern computer aided design/computer aided manufacturing systems using WEDM.

Yang *et al.* [19] used a mechanism for the propagation of acoustic emission (AE) and present a new labeling method along with an effective deep learning dual-input model called batch relevance temporal convolution neural network based on the analysis of collected signals. A relationship between AE and pulse time series was studied. Saha *et al.* [20] examined the machining of composite material made of tungsten carbide–cobalt where artificial neural network (ANN) models were used to predict the surface roughness and cutting speed. Singh and Misra [21] highlighted that the backpropagation neural network (BPNN) in the ANN toolset was an efficient technique for surface roughness prediction during WEDM. Soni *et al.* [22] have proved that ANN-predicted surface roughness and material removal rate were closer to the experiments during WEDM of Ti–Ni–Co shape memory alloy. Manoj and Narendranath [23] have used ANN prediction for forecasting the profile areas in slant-type tapering operation during WEDM of Hastelloy-X.

From the literature, it can be concluded that many parameters influence the accuracy of the profile. In the literature, we can observe that most of the experiments overcut surface roughness and cutting speed with traditional parameters such as pulse on, pulse off, wire tension, wire speed, servo voltage, and so on. There are other parameters that influence the overall area; in the present investigation, different effects of parameters such as CO, profile offset (PO), dwell time (DT), and wire distance (WD) on the areas of the holes were analyzed. A fixture is used for machining taper holes at 0°, 15°, and 30° taper angles. It was seen that DT did not affect the areas of the holes. As the WD between guides increased, the area of the holes decreased contrastingly, and the increase in PO increased the area. ANN was used to automate the process by predicting the areas at different taper angles for the various parameters by removing human interference in experimentation and characterization.

## 2 Materials

Nickelvac-HX is a type of nickel superalloy that boasts exceptional mechanical properties, making it a popular choice for a wide range of applications. This alloy is commonly used in the manufacture of combustor cans, spray bars, flame holders, afterburners, tailpipes, dyes, and metal stampings, among other uses. The alloy was heated to 2,150°F (1,177°C) and rapidly cooled as heat treatment (The solution annealing of 1 hr per inch of the section was followed) [24]. After the heat treatment process, the plate was machined to 260 mm × 22 mm × 10 mm dimensions.

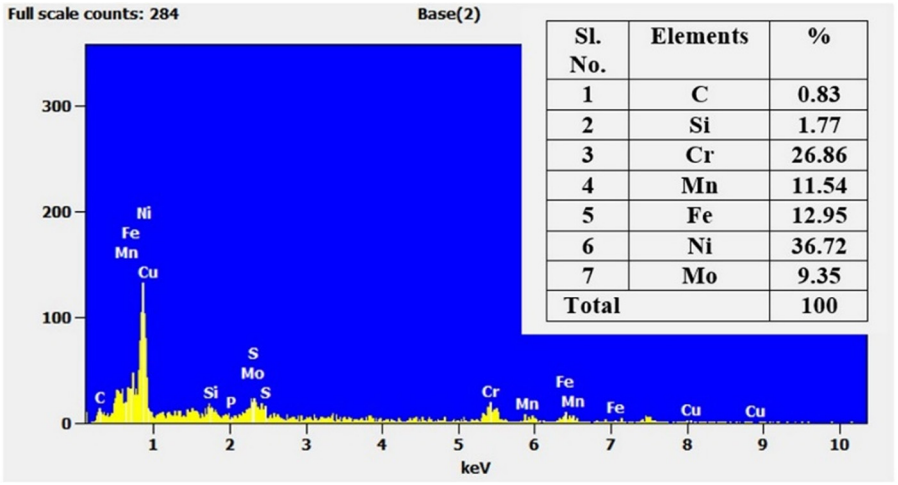


| Sl. No. | Elements | % |
|---|---|---|
| 1 | C | 0.83 |
| 2 | Si | 1.77 |
| 3 | Cr | 26.86 |
| 4 | Mn | 11.54 |
| 5 | Fe | 12.95 |
| 6 | Ni | 36.72 |
| 7 | Mo | 9.35 |
| Total | | 100 |

**Figure 1:** EDS graph of the Nickelvac-HX.

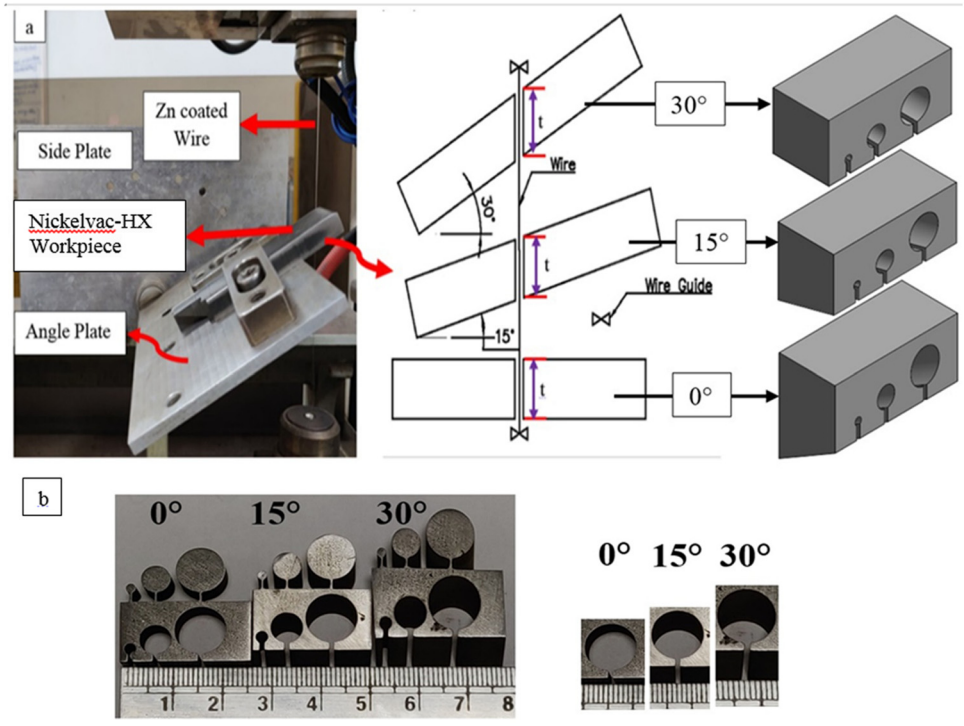


**Figure 2:** (a) Slant fixture on WEDM table at 0°, 15°, and 30° angular positions and components after machining. (b) Machined components.

The measurement of the elements and their percentage in the material using energy dispersive spectroscopy (EDS) technique is shown in Figure 1. This was then fixed to the fixture for machining as shown in Figure 2. Similar experiments with fixture for tapering were also conducted in Manoj *et al.* [14,15,23].

## 3 Experimental setup and design

The "ELPULS 15 CNC WEDM" from Electronica, Pune, was used to machine Nickelvac-HX. Throughout the experiment, the dielectric fluid was deionized water and the electrode was a zinc-coated copper wire of 0.25 mm in diameter. The

**Table 1:** EDM parameters used for machining

| EDM parameters | | Settings (levels) | | | |
|---|---|---|---|---|---|
| Wire distance between guides(mm) (WD) | 0° | 40 | 50 | 60 | 70 |
| | 15° | 75 | 85 | 95 | 105 |
| | 30° | 100 | 110 | 120 | 130 |
| Profile offset (microns) (PO) | | 0 | 40 | 80 | 120 |
| Cutting-speed override (%) (CO) | | 31 | 54 | 77 | 100 |
| Dwell time (s) (DT) | | 0 | 33 | 66 | 99 |

circular hole was programmed using numerically controlled codes for different PO. These are converted into WC files for the necessary machining conditions by the computer numerical control (CNC) profiling software called ELCAM. The WC files were instructions for the machine for profiling with specific conditions such as shape, distance, offset, and curvature. This WC file is loaded to the CNC-controlled WEDM. The slant-type taper fixture was fixed to the WEDM bed where the workpiece was fixed to the fixture as shown in Figure 2(a). It also shows the movement of the angular plate to achieve the required angle during machining and different workpieces after machining. Different dimensions of slant holes namely 1, 3, and 5 mm were machined as shown in Figure 2(b). As WEDM is a complex process, among different parameters, a suitable parameter setting has to be found. The machine parameters were fixed during the experimentation so that machining occurs at all the taper angles: Pulse-off time = 44 µs, corner control = 3%, wire speed = 6 m/min, servo feed = 20 mm/min, servo voltage = 40 V, pulse-on time = 115 µs, and flushing pressure = 0 kg/cm². Table 1 indicates the profiling parameters. These machining parameters were selected based on the preliminary experiments, machining range, and fixture angles so that the profiling can be easily carried out.

## 4 Characterization process

The machined components were measured by "Hitachi SU 3500" and "JEO JSM-6368OLA" scanning electron microscope (SEM) and "TESA VISIO 200"-made coordinate measuring machine (CMM). The machined holes were characterized differently as indicated in Figure 3. The 1 mm hole images were taken using SEM. Furthermore, the SEM images were imported into ImageJ software for measuring the diameter and calculating the areas. The 3 and 5 mm holes were measured using CMM. As the hole dimension changes in different taper angles, we have taken the areas of the hole as output parameters. The areas of taper profiles were calculated, and a similar characterization was followed for all the holes. The 3 mm profile was neglected as it showed the same effect as 1 mm and 5 mm. ANN toolbox was used for prediction using MATLAB software.

## 5 Results and discussion

The areas of the hole were machined for various parameters at different taper angles as shown in Table 2. It can be seen that the highest areas of the hole were found at 100% PO. Although the cutting parameters were the same, the difference in profiling parameters leads to variations in areas.

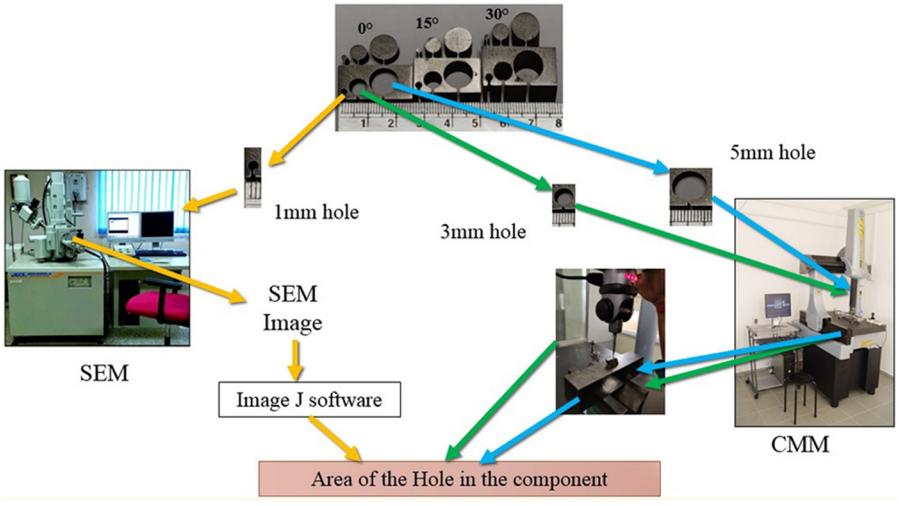


**Figure 3:** Measurement of the different holes in the component.

**Table 2:** Variation of areas of holes at different taper angles

| Sl. no. | WD (mm) | DT (s) | PO (µm) | CO (%) | Area of holes in mm² | |
|---|---|---|---|---|---|---|
| | | | | | 1 mm | 5 mm |
| **0° Taper angle** | | | | | | |
| 1 | 40 | 0 | 0 | 31 | 4.568 | 84.961 |
| 2 | 40 | 33 | 40 | 54 | 4.800 | 85.576 |
| 3 | 40 | 66 | 80 | 77 | 4.966 | 87.059 |
| 4 | 40 | 99 | 120 | 100 | 5.060 | 87.516 |
| 5 | 50 | 0 | 40 | 77 | 4.651 | 85.363 |
| 6 | 50 | 33 | 0 | 100 | 4.351 | 83.801 |
| 7 | 50 | 66 | 120 | 31 | 5.166 | 87.964 |
| 8 | 50 | 99 | 80 | 54 | 4.920 | 86.701 |
| 9 | 60 | 0 | 80 | 100 | 4.781 | 85.936 |
| 10 | 60 | 33 | 120 | 77 | 4.813 | 85.487 |
| 11 | 60 | 66 | 0 | 54 | 4.297 | 84.057 |
| 12 | 60 | 99 | 40 | 31 | 4.611 | 84.655 |
| 13 | 70 | 0 | 120 | 54 | 4.819 | 86.132 |
| 14 | 70 | 33 | 80 | 31 | 4.759 | 85.944 |
| 15 | 70 | 66 | 40 | 100 | 4.312 | 83.243 |
| 16 | 70 | 99 | 0 | 77 | 4.198 | 82.755 |
| **15° Taper angle** | | | | | | |
| 1 | 75 | 0 | 0 | 31 | 6.068 | 87.961 |
| 2 | 75 | 33 | 40 | 54 | 6.310 | 88.776 |
| 3 | 75 | 66 | 80 | 77 | 6.386 | 89.729 |
| 4 | 75 | 99 | 120 | 100 | 6.580 | 90.616 |
| 5 | 85 | 0 | 40 | 77 | 6.111 | 88.233 |
| 6 | 85 | 33 | 0 | 100 | 5.871 | 86.971 |
| 7 | 85 | 66 | 120 | 31 | 6.606 | 90.904 |
| 8 | 85 | 99 | 80 | 54 | 6.330 | 89.171 |
| 9 | 95 | 0 | 80 | 100 | 6.241 | 88.536 |
| 10 | 95 | 33 | 120 | 77 | 6.343 | 88.787 |
| 11 | 95 | 66 | 0 | 54 | 5.767 | 87.027 |
| 12 | 95 | 99 | 40 | 31 | 6.109 | 87.755 |
| 13 | 105 | 0 | 120 | 54 | 6.319 | 89.032 |
| 14 | 105 | 33 | 80 | 31 | 6.229 | 88.944 |
| 15 | 105 | 66 | 40 | 100 | 5.801 | 86.313 |
| 16 | 105 | 99 | 0 | 77 | 5.698 | 85.855 |
| **30° Taper angle** | | | | | | |
| 1 | 100 | 0 | 0 | 31 | 8.068 | 92.756 |
| 2 | 100 | 33 | 40 | 54 | 8.100 | 96.099 |
| 3 | 100 | 66 | 80 | 77 | 8.426 | 97.940 |
| 4 | 100 | 99 | 120 | 100 | 8.520 | 100.462 |
| 5 | 110 | 0 | 40 | 77 | 7.951 | 92.914 |
| 6 | 110 | 33 | 0 | 100 | 7.851 | 89.993 |
| 7 | 110 | 66 | 120 | 31 | 8.626 | 100.848 |
| 8 | 110 | 99 | 80 | 54 | 8.380 | 97.102 |
| 9 | 120 | 0 | 80 | 100 | 8.231 | 95.769 |
| 10 | 120 | 33 | 120 | 77 | 8.263 | 97.097 |
| 11 | 120 | 66 | 0 | 54 | 7.707 | 88.230 |
| 12 | 120 | 99 | 40 | 31 | 7.811 | 92.872 |
| 13 | 130 | 0 | 120 | 54 | 8.319 | 96.535 |
| 14 | 130 | 33 | 80 | 31 | 8.259 | 95.786 |
| 15 | 130 | 66 | 40 | 100 | 7.672 | 88.240 |
| 16 | 130 | 99 | 0 | 77 | 7.658 | 87.201 |

## 5.1 Analysis of variance (ANOVA) and main effect plot

The Variation of areas of holes at different taper angles is as shown in Table 2. Table 3 shows the ANOVA, and Figures 4–6 show the main effect plots. From the table and figures, it can be noticed that WD and PO were the most influencing factors in the area of the hole. The PO parameter has the highest % contribution of 67.2–78.2%, making it the most important parameter. Furthermore, WD parameter has a % contribution of 18.1–23.3%. It was then followed by the CO parameter, making it the least effective parameter. It can also be seen that WD and PO were the only significant factors compared to other parameters. The main effect plot and ANOVA indicate that the DT parameter has no role in influencing the areas of the hole. As the DT parameter is the dwell time parameter, it gets activated at the sharp edges. This parameter stops in an edge coordinate before the next command [14,24]. This reduces the wire bend errors, especially the corner errors. In the profile, there are no edges as it is a hole, so the DT parameter becomes the least effective. The DT parameter depends on the geometry of the profile also. Small variations such as increase and decrease were spotted in the main effect plot due to the vibrations, as stated by Habib [25]. Similar results were obtained by Manoj and Narendranath and Soni *et al.* [14,22] for circular profile areas. So the DT parameter is neglected for further investigation.

### 5.1.1 Influence of WD parameter on the area of the hole

The next significant factor affecting the areas of the holes is the WD parameter. It controls the wire distance between the two guides during machining. It becomes important when cutting taper complex profiles. From the effect plot, we can see that as the WD parameter escalates, the area of the hole decreases. However, as the length of the wire increases during machining, it decreases the tension in the wire, which induces wire bending. The bending of this wire causes a lag affecting the area of the holes machined [26]. Figures 5(a) and 6(b) show a decrease in areas of the profile as the WD parameter increases. It was noticed in the remaining graphs that there were small variations in decrease because of the wire vibration. Chaudhary *et al.* [27] reported that as the wire length escalates, the tension in the wire decreases; this decrease in the tension of the wire leads to wire vibration.

**Table 3:** ANOVA

| Sl. no. | Parameters | Degree of freedom | Areas 1 mm² hole | | Areas 5 mm² hole | |
|---|---|---|---|---|---|---|
| | | | Adjacent sum of squares | Contribution in % | Adjacent sum of squares | Contribution in % |
| **0° Taper angle** | | | | | | |
| **1** | **WD** | **3** | **0.263** | **18.119** | **53.431** | **19.705** |
| 2 | DT | 3 | 0.005 | 0.367 | 1.860 | 0.686 |
| **3** | **PO** | **3** | **1.137** | **78.273** | **203.659** | **75.109** |
| 4 | CO | 3 | 0.039 | 2.663 | 9.403 | 3.468 |
| 5 | Error | 3 | 0.008 | 0.577 | 2.797 | 1.032 |
| **15° Taper angle** | | | | | | |
| **1** | **WD** | **3** | **0.236** | **20.738** | **7.279** | **24.309** |
| 2 | DT | 3 | 0.006 | 0.534 | 0.053 | 0.176 |
| **3** | **PO** | **3** | **0.843** | **73.993** | **20.129** | **67.219** |
| 4 | CO | 3 | 0.042 | 3.650 | 1.589 | 5.306 |
| 5 | Error | 3 | 0.012 | 1.085 | 0.895 | 2.990 |
| **30° Taper angle** | | | | | | |
| **1** | **WD** | **3** | **0.263** | **18.119** | **53.431** | **19.705** |
| 2 | DT | 3 | 0.005 | 0.367 | 1.860 | 0.686 |
| **3** | **PO** | **3** | **1.137** | **78.273** | **203.659** | **75.109** |
| 4 | CO | 3 | 0.039 | 2.663 | 9.403 | 3.468 |
| 5 | Error | 3 | 0.008 | 0.577 | 2.797 | 1.032 |

The bold values indicates that WD is the least contribution and PO is the highest contribution.

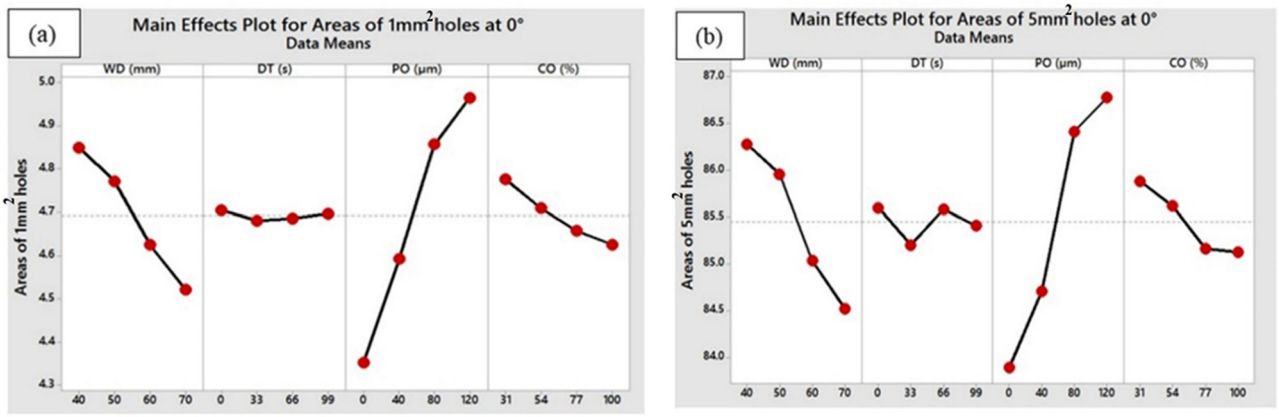


**Figure 4:** Effect plot at 0° for (a) 1 mm and (b) 5 mm holes.

### 5.1.2 Influence of CO parameter on the area of the hole

The CO is an online parameter that controls the cutting speed during machining of the hole. This CO parameter aids in the machining of complex geometrical profiles at different taper angles. It wheels the cutting speed by controlling the discharge energy generated during machining. This is also called an online parameter as it alters the discharge energy instantaneously during machining based on the geometry of the profile and machining conditions. It avoids wire breaks during the complex machining process [14,24]. As the CO parameter increases, it was seen that the area of the hole decreases, as observed clearly in Figures 4(a), 5(a) and 6(a and b). This is because as the CO increases, the cutting speed also increases. Higher cutting speed results in wire lag as the wire does not travel accurately to the specific coordinates. So this lag in the wire induced by the cutting speed decreases the areas of the holes. Manoj and Narendranath and Soni *et al.* [14,22] also observed a similar phenomenon in their study. There were small decreases in main effect graphs due to the vibrations caused by instantaneous changes in cutting speed [28].

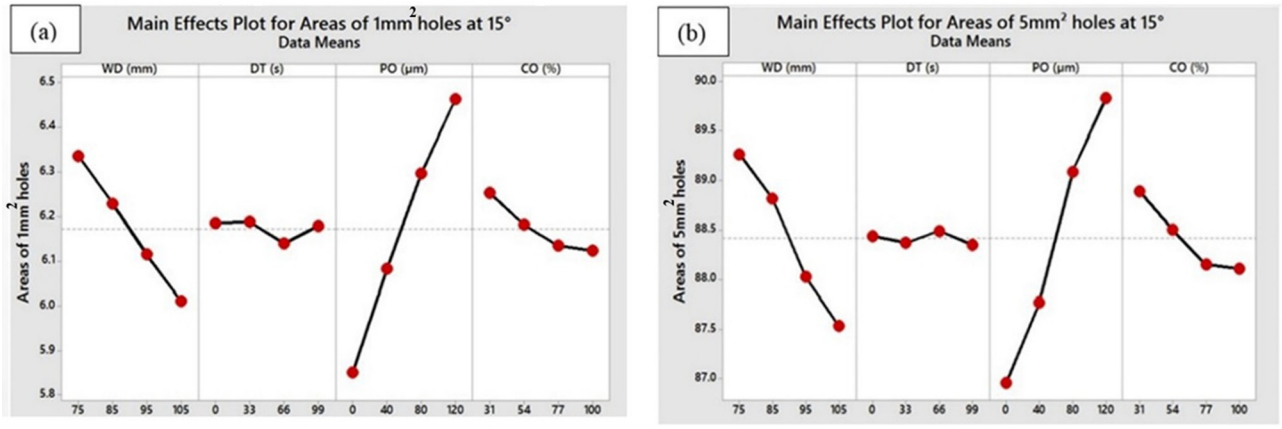


**Figure 5:** Effect plot at 15° for (a) 1 mm and (b) 5 mm holes.

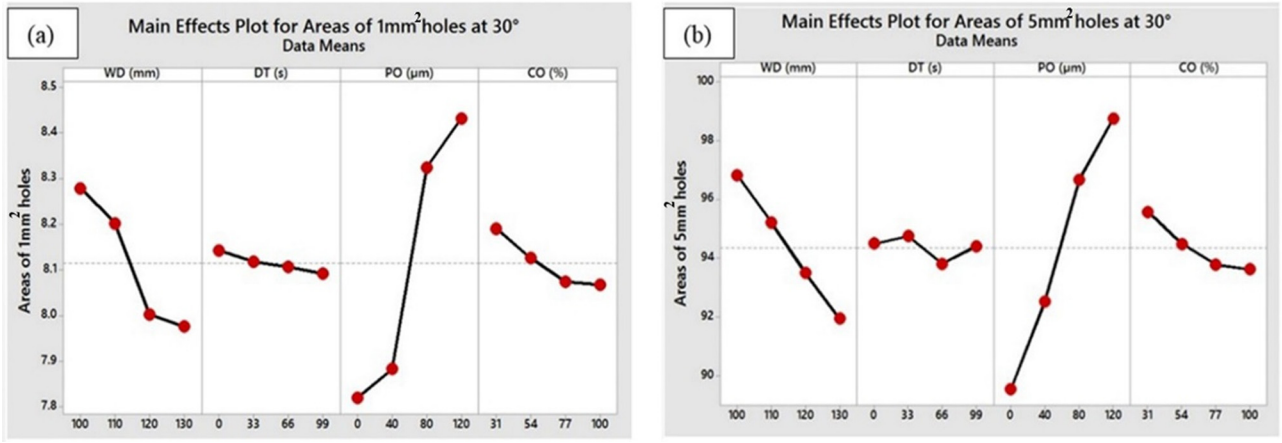


**Figure 6:** : Effect plot at 30° for (a) 1 mm and (b) 5 mm holes.

## 5.2 Variation of taper areas of the hole at different taper angles

Figure 7 shows the variation in the area of holes at different taper angles. As the taper angle escalates, the area of the hole also increases. This trend was also observed in 1, 3, and 5 mm holes. It can be seen at various profiling parameters (experimental trials) that at 30° taper angles the areas were the highest, and at 0° taper angles, the areas were the lowest. The 15° taper angles always remained in between them. This phenomenon was noticed because of the taper provided by the fixture during machining as shown in Figure 2(b). The material available at taper or slant (15° and 30°) machining is higher compared to horizontal machining (0°). It can be seen that as the taper angle increases, the workpiece also tilts with respect to the wire. The wire path which is programmed remains the same, and the material is given an angle with the help of fixture. This increases the material available for machining which in turn increases the surface area. As the material availability increases, the areas of the hole also increase. Manoj and Narendranath and Soni *et al.* [14,22] also noted similar results during slant profiling.

## 5.3 ANN

An ANN, which is the foundation for artificial intelligence (AI), was used for the statistical prediction of areas of holes. The 48 experimental trials conducted at various parameters in all three taper angles were made use for the prediction. The DT parameters were neglected in

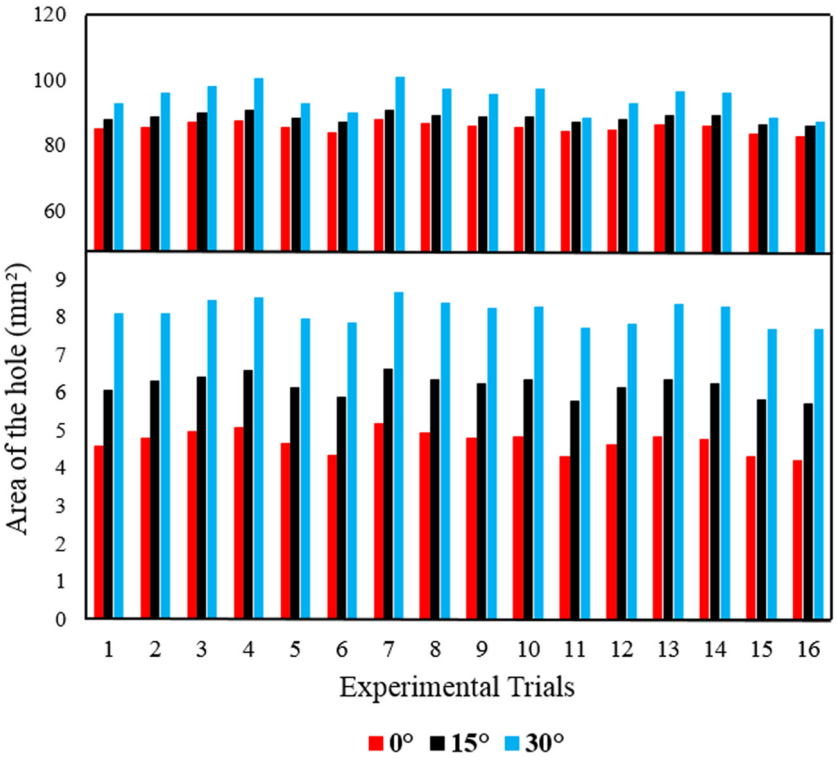


**Figure 7:** Areas of the holes at different taper angles.

prediction as they have very little effect on the areas of the holes machined. The MATLAB ANN tool distributes the data for training, validation, and testing in the ratio of 70, 15, and 15% for ANN modeling, respectively. Ghosh *et al.* [29] stated that BPNN with Levenberg–Marquardt algorithm is the most efficient method. The 5-9-1-1 architecture was the most optimal neural network found for predictions. The output responses were normalized from 1 to –1. The functions tansig and pureline were used for modeling the neural network. Table 4 shows the measured and predicted areas at different parameters.

### 5.4 Validation of optimum model

From the optimal ANN model that was developed, it can be seen from Table 4 that the prediction of the experimental parameter has an error ranging from 0 to 5%. The validation was performed to outline the behavior of the ANN model beyond the parameters used for training, testing, and validation. The parameters were randomly chosen as shown in Table 5 and it was input into the ANN model. This was experimentally compared by a similar characterization method. The error of 0–8% is shown in Table 5. The model not only gives the areas but also helps to decide the optimal parameters based on the parametric behavior. As the output of different parameters can be predicted without experimentation. For evaluation of the ANN model, the mean square error, mean absolute error, and root mean square error of 1 mm profile were 0.03, 0.0034, and 0.06 and for 5 mm profile were 0.48, 0.99, and 1.00, respectively.

## 6 Conclusion

The parametric variation was outlined by machining holes at different taper angles on Nickelvac-HX. The ANN, which is one of the AI techniques, acts as a predictor and an automation tool for the set of parameters. Here, it is used as an automation tool as it gives the area of the hole for a defined set of parameters without experimentation and avoiding human intervention. The following conclusions were drawn:

- As the PO parameter increases from 0 to 40 µm, the area of the holes increases from 3.32 to 12.3% which proves that it is the most influential on the area of the hole. The DT parameter has no significant effect on the areas.

**Table 4:** Prediction and measured areas from the ANN model

| Taper angle (degree) | Sl. no. | WD (mm) | PO (μm) | CO (%) | Predicted area of hole (mm²) | | Measured area of hole (mm²) | | (% Error) (%) | |
|---|---|---|---|---|---|---|---|---|---|---|
| | | | | | 1 mm | 5 mm | 1 mm | 5 mm | 1 mm | 5 mm |
| 0° | 1 | 40 | 0 | 31 | 4.614 | 84.961 | 4.568 | 84.961 | 1.01 | 0.00 |
| | 2 | 40 | 40 | 54 | 4.822 | 85.366 | 4.800 | 85.576 | 0.46 | 0.25 |
| | 3 | 40 | 80 | 77 | 4.972 | 88.999 | 4.966 | 87.059 | 0.12 | 2.18 |
| | 4 | 40 | 120 | 100 | 5.065 | 87.481 | 5.060 | 87.516 | 0.10 | 0.04 |
| | 5 | 50 | 40 | 77 | 4.651 | 84.898 | 4.651 | 85.363 | 0.00 | 0.55 |
| | 6 | 50 | 0 | 100 | 4.323 | 83.816 | 4.351 | 83.801 | 0.64 | 0.02 |
| | 7 | 50 | 120 | 31 | 5.130 | 88.311 | 5.166 | 87.964 | 0.70 | 0.39 |
| | 8 | 50 | 80 | 54 | 4.916 | 86.522 | 4.920 | 86.701 | 0.08 | 0.21 |
| | 9 | 60 | 80 | 100 | 4.698 | 85.768 | 4.781 | 85.936 | 1.74 | 0.20 |
| | 10 | 60 | 120 | 77 | 4.866 | 85.503 | 4.813 | 85.487 | 1.10 | 0.02 |
| | 11 | 60 | 0 | 54 | 4.294 | 83.895 | 4.297 | 84.057 | 0.07 | 0.19 |
| | 12 | 60 | 40 | 31 | 4.637 | 84.818 | 4.611 | 84.655 | 0.56 | 0.19 |
| | 13 | 70 | 120 | 54 | 4.807 | 90.579 | 4.819 | 86.132 | 0.25 | 4.91 |
| | 14 | 70 | 80 | 31 | 4.700 | 85.906 | 4.759 | 85.944 | 1.24 | 0.04 |
| | 15 | 70 | 40 | 100 | 4.418 | 83.394 | 4.312 | 83.243 | 2.46 | 0.18 |
| | 16 | 70 | 0 | 77 | 4.132 | 82.481 | 4.198 | 82.755 | 1.57 | 0.33 |
| 15° | 17 | 75 | 0 | 31 | 6.055 | 88.097 | 6.068 | 87.961 | 0.21 | 0.15 |
| | 18 | 75 | 40 | 54 | 6.290 | 91.990 | 6.310 | 88.776 | 0.32 | 3.49 |
| | 19 | 75 | 80 | 77 | 6.432 | 89.886 | 6.386 | 89.729 | 0.72 | 0.17 |
| | 20 | 75 | 120 | 100 | 6.556 | 90.357 | 6.580 | 90.616 | 0.36 | 0.29 |
| | 21 | 85 | 40 | 77 | 6.112 | 88.314 | 6.111 | 88.233 | 0.02 | 0.09 |
| | 22 | 85 | 0 | 100 | 5.851 | 86.936 | 5.871 | 86.971 | 0.34 | 0.04 |
| | 23 | 85 | 120 | 31 | 6.587 | 90.969 | 6.606 | 90.904 | 0.29 | 0.07 |
| | 24 | 85 | 80 | 54 | 6.367 | 89.196 | 6.330 | 89.171 | 0.58 | 0.03 |
| | 25 | 95 | 80 | 100 | 6.168 | 88.585 | 6.241 | 88.536 | 1.17 | 0.06 |
| | 26 | 95 | 120 | 77 | 6.388 | 88.794 | 6.343 | 88.787 | 0.71 | 0.01 |
| | 27 | 95 | 0 | 54 | 5.768 | 86.829 | 5.767 | 87.027 | 0.02 | 0.23 |
| | 28 | 95 | 40 | 31 | 6.090 | 85.994 | 6.109 | 87.755 | 0.31 | 2.05 |
| | 29 | 105 | 120 | 54 | 6.331 | 88.911 | 6.319 | 89.032 | 0.19 | 0.14 |
| | 30 | 105 | 80 | 31 | 6.225 | 89.152 | 6.229 | 88.944 | 0.06 | 0.23 |
| | 31 | 105 | 40 | 100 | 5.851 | 86.093 | 5.801 | 86.313 | 0.86 | 0.26 |
| | 32 | 105 | 0 | 77 | 5.542 | 85.977 | 5.698 | 85.855 | 2.74 | 0.14 |
| 30° | 33 | 100 | 0 | 31 | 8.034 | 90.845 | 8.068 | 92.756 | 0.42 | 2.10 |
| | 34 | 100 | 40 | 54 | 8.187 | 96.029 | 8.100 | 96.099 | 1.07 | 0.07 |
| | 35 | 100 | 80 | 77 | 8.407 | 98.370 | 8.426 | 97.940 | 0.23 | 0.44 |
| | 36 | 100 | 120 | 100 | 8.542 | 101.898 | 8.520 | 100.462 | 0.26 | 1.41 |
| | 37 | 110 | 40 | 77 | 7.998 | 93.440 | 7.951 | 92.914 | 0.59 | 0.56 |
| | 38 | 110 | 0 | 100 | 7.803 | 89.874 | 7.851 | 89.993 | 0.61 | 0.13 |
| | 39 | 110 | 120 | 31 | 8.634 | 100.854 | 8.626 | 100.848 | 0.09 | 0.01 |
| | 40 | 110 | 80 | 54 | 8.341 | 97.402 | 8.380 | 97.102 | 0.47 | 0.31 |
| | 41 | 120 | 80 | 100 | 8.140 | 93.998 | 8.231 | 95.769 | 1.11 | 1.88 |
| | 42 | 120 | 120 | 77 | 8.339 | 97.310 | 8.263 | 97.097 | 0.92 | 0.22 |
| | 43 | 120 | 0 | 54 | 7.731 | 88.526 | 7.707 | 88.230 | 0.31 | 0.33 |
| | 44 | 120 | 40 | 31 | 7.954 | 93.275 | 7.811 | 92.872 | 1.83 | 0.43 |
| | 45 | 130 | 120 | 54 | 8.282 | 96.664 | 8.319 | 96.535 | 0.44 | 0.13 |
| | 46 | 130 | 80 | 31 | 8.124 | 95.552 | 8.259 | 95.786 | 1.63 | 0.24 |
| | 47 | 130 | 40 | 100 | 7.731 | 88.287 | 7.672 | 88.240 | 0.77 | −0.05 |
| | 48 | 130 | 0 | 77 | 7.606 | 87.191 | 7.658 | 87.201 | −0.68 | 0.01 |

**Table 5:** Validation of the optimum ANN model

| Sl. no. | WD (mm) | PO (μm) | CO (%) | Taper angle (degree) | 1 mm hole | | | 5 mm hole | | |
|---|---|---|---|---|---|---|---|---|---|---|
| | | | | | ANN-predicted areas ($mm^2$) | Measured areas ($mm^2$) | Error (%) | ANN-predicted areas ($mm^2$) | Measured areas ($mm^2$) | Error (%) |
| 1 | 55 | 100 | 45 | 0 | 4.943 | 4.769 | 3.530 | 87.369 | 86.994 | 0.429 |
| 2 | 80 | 180 | 80 | 0 | 4.884 | 5.196 | 6.383 | 70.013 | 71.222 | 1.726 |
| 3 | 90 | 75 | 65 | 15 | 6.264 | 6.008 | 4.091 | 88.639 | 91.567 | 3.303 |
| 4 | 120 | 150 | 50 | 15 | 6.329 | 6.828 | 7.877 | 79.786 | 75.998 | 4.748 |
| 5 | 115 | 50 | 90 | 30 | 8.001 | 7.856 | 1.814 | 92.798 | 87.945 | 5.229 |
| 6 | 145 | 130 | 70 | 30 | 8.095 | 8.456 | 4.461 | 92.075 | 94.256 | 2.369 |

- The WD is the next significant factor; as it increases, the areas increase from 2.04 to 6.73%, and the CO parameter is seen to affect the areas of the hole to the least extent as % contribution also varies from 2.66 to 5.30%.
- As the taper angle escalates from 0° to 30°, the areas of the holes also increase from 9.70 to 82.41%.
- The ANN model showed that errors are ranging up to 8% in prediction during validation by experimentation.
- Similar research could be carried out for several additional materials and manufacturing processes as future work. Furthermore, as AI models can improve over time by being trained on new datasets, such algorithms can be used for additional prediction and process control.

**Funding information:** The author states no funding involved.

**Author contributions:** Manoj IV and Narendranath S wrote the article.The rest of the authors reviewed, edited, and acquired the funding for the manuscript.

**Conflict of interest:** Authors state no conflict of interest.

**Informed consent:** Informed consent was obtained from all individuals included in this study.

**Ethical approval:** The conducted research is not related to either human or animals use.

**Data availability statement:** Data sharing is not applicable to this article, as no datasets were generated during the research work.

# References

[1] P. Kulkarni and S. Chinchanikar, "A review on machining of nickel-based superalloys using nanofluids under minimum quantity lubrication (NFMQL)," *J. Inst. Eng. India Ser. C.*, vol. 104, pp. 183–199, 2023.

[2] I. V. Manoj and S. Narendranath, "Evaluation of WEDM performance characteristics and prediction of machining speed during taper square profiling on Hastelloy-X," *Aust. J. Mech. Eng.*, 2021. doi: 10.1080/14484846.2021.1960670.

[3] H. Soni, S. Narendranath, and M. R. Ramesh, "Experimental investigation on effects of wire electro discharge machining of $Ti_50Ni_{45}Co_5$ shape memory alloys," *Silicon*, vol. 10, pp. 2483–2490, 2018.

[4] K. K. Goyal, N. Sharma, R. D. Gupta, S. Gupta, D. Rani, D. Kumar, et al., "Measurement of performance characteristics of WEDM while processing AZ31 Mg-alloy using Levy flight MOGWO for orthopedic application," *Int. J. Adv. Manuf. Technol.*, vol. 119, pp. 7175–7197, 2022.

[5] K. Mouralova, L. Benes, J. Bednar, R. Zahradnicek, T. Prokes, R. Matousek, et al., "Using a DoE for a comprehensive analysis of the surface quality and cutting speed in WED-machined hadfield steel," *J. Mech. Sci. Technol.*, vol. 33, pp. 2371–2386, 2019.

[6] W. Ming, C. Cao, F. Shen, Z. Zhang, K. Liu, J. Du, et al., "Numerical and experimental study on WEDM of BN-AlN-$TiB_2$ composite ceramics based on a fusion FEM model," *J. Manuf. Process*, vol. 76, pp. 138–154, 2022.

[7] W. He, S. He, J. Du, W. Ming, J. Ma, Y. Cao, et al., "Fiber orientations effect on process performance for wire cut electrical discharge machining (WEDM) of 2D C/SiC composite," *Int. J. Adv. Manuf. Technol.*, vol. 102, pp. 507–518, 2019.

[8] S. Wang, J. Wu, H. Gunawan, and R. Tu, "Optimization of Machining Parameters for Corner Accuracy Improvement for WEDM Processing," *Appl. Sci.*, vol. 12, no. 20, pp. 1–10, 2022.

[9] N. Kinoshita, M. Fukui, and T. Fujii, "Study on wire-EDM: Accuracy in Taper-Cut," *Ann. CIRP.*, vol. 36, pp. 119–122, 1987.

[10] S. Y. Martowibowo and A. Wahyudi, "Taguchi method implementation in taper motion wire EDM process optimization," *J. Inst. Eng. India Ser. C.*, vol. 93, pp. 357–364, 2012.

[11] H. Yan, Z. Liu, L. Li, C. Li, and X. He, "Large taper mechanism of HS-WEDM," *Int. J. Adv. Manuf. Technol.*, vol. 90, pp. 2969–2977, 2017.

[12] J. A. Sanchez, S. Plaza, N. Ortega, M. Marcos, and J. Albizuri, "Experimental and numerical study of angular error in WEDM taper–cutting," *Int. J. Mach. Tools Manuf.*, vol. 48, pp. 1420–1428, 2008.

[13] R. Joy, I. V. Manoj, and S. Narendranath, "Investigation of cutting speed, recast layer and micro-hardness in angular machining using slant type taper fixture by WEDM of Hastelloy X," *Mater. Today*, vol. 27, pp. 1943–1946, 2019.

[14] I. V. Manoj and S. Narendranath, "Slant type taper profiling and prediction of profiling speed for a circular profile during in wire electric discharge machining using Hastelloy-X," *Proc. Inst. Mech. Eng. C. J. Mech Eng Sci.*, vol. 235, no. 2, pp. 341–353, 2021. doi: 10.1177/0954406221992398.

[15] I. V. Manoj and S. Narendranath, "Parametric analysis and response surface optimization of surface roughness and cutting rate in the machining using WEDM," *Lecture Notes in Mechanical Engineering*, Springer Nature, Singapore, 2021, pp. 143–150. doi: 10.1007/978-981-16-4138-1_14.

[16] H. Abyar, A. Abdullah, and A. Akbarzadeh, "Analyzing wire deflection errors of WEDM process on small arced corners," *J. Manuf. Process*, vol. 36, pp. 216–223, 2018. doi: 10.1016/j.jmapro.2018.09.011.

[17] H. Bisaria and P. Shandilya, "Processing of curved profiles on Ni-rich nickel–titanium shape memory alloy by WEDM," *Mater. Manuf. Process*, vol. 34, no. 13, pp. 1333–1341, 2019. doi: 10.1080/10426914.2019.1603521.

[18] A. Werner, "Method for enhanced accuracy in machining curvilinear profiles on wire-cut electrical discharge machines," *Precis. Eng.*, vol. 44, pp. 75–80, 2016. doi: 10.1016/j.precisioneng.2015.08.001.

[19] X. Yang, C. Liu, L. Peng, S. Peng, Y. Zhang, N. Xie, et al., "A new BRTCN model for predicting discharge status of WEDM based on acoustic emission," *J. Manuf. Syst.*, vol. 64, pp. 409–423, 2022. doi: 10.1016/j.jmsy.2022.07.005.

[20] P. Saha, A. Singh, S. K. Pal, and P. Saha, "Soft computing models based prediction of cutting speed and surface roughness in wire electro-discharge machining of tungsten carbide cobalt composite," *Int. J. Adv. Manuf. Technol.*, vol. 39, pp. 74–84, 2008.

[21] B. Singh and J. P. Misra, "Surface finish analysis of wire electric discharge machined specimens by RSM and ANN modelling," *J. Int. Meas. Confed.*, vol. 137, pp. 225–237, 2019. doi: 10.1016/j.measurement.2018.07.020.

[22] H. Soni, S. Narendranath, and M. R. Ramesh, "ANN and RSM modeling methods for predicting material removal rate and surface roughness during WEDM of $Ti_50Ni_40Co_{10}$ shape memory alloy," *Adv. Model. Anal. A.*, vol. 54, no. 6, pp. 435–443, 2017. doi: 10.1007/s10462-017-9546-4.

[23] I. V. Manoj and S. Narendranath, "Variation and artificial neural network prediction of profile areas during slant type taper profiling of triangle at different machining parameters on Hastelloy X by wire electric discharge machining," *Proc. Inst. Mech. Eng. E J. Process. Mech. Eng.*, vol. 234, no. 4, pp. 673–683, 2020. doi: 10.1177/0954408920920789.

[24] H. Chandler, *Heat treater's guide practices and procedures for ferrous alloys*, ASM International, United States of America, 2006.

[25] S. Habib, "Optimization of machining parameters and wire vibration in wire electrical discharge machining process," *Mech. Adv. Mater. Mod. Process*, vol. 3, no. 3, 2017. doi: 10.1186/s40759-017-0017-1.

[26] B. E. Z. Read and B. A. Zenyth, *Operating Manual for ELPLUS 15 Ecocut*, 2011. Retrieved by email from company, access date: 25 May 2011.

[27] T. Chaudhary, A. N. Siddiquee, and A. K. Chanda, "Effect of wire tension on different output responses during wire electric discharge machining on AISI 304 stainless steel," *Def. Technol.*, vol. 15, pp. 541–544, 2019.

[28] S. Habib and A. Okada, "Experimental investigation on wire vibration during fine wire electrical discharge machining process," *Int. J. Adv. Manuf. Technol.*, vol. 84, pp. 2265–2276, 2016.

[29] G. Ghosh, P. Mandal, and S. C.Mondal, "Modeling and optimization of surface roughness in keyway milling using ANN, genetic algorithm, and particle swarm optimization," *Int. J. Adv. Manuf. Technol.*, vol. 100, pp. 1223–1242, 2019.